Palladium Chemistry in Molten Alkali Metal Polychalcophosphate Fluxes. Synthesis and Characterization of $K_4Pd(PS_4)_2$, $Cs_4Pd(PSe_4)_2$, $Cs_{10}Pd(PSe_4)_4$, $KPdPS_4$, $K_2PdP_2S_6$, and $Cs_2PdP_2Se_6$

Konstantinos Chondroudis and Mercouri G. Kanatzidis*

Department of Chemistry, Michigan State University, East Lansing, Michigan 48824

Julien Sayettat, Stéphane Jobic, and Raymond Brec*

Institut des Matériaux de Nantes, B.P. 32229, 44322 Nantes Cedex 03, France

Received May 16, 1997[⊗]

The reaction of Pd with a molten mixture of $A_2Q_x/P_2Q_5/Q$ (A = K, Q = S, x = 3; A = Cs, Q = Se, x = 1) produced the molecular compounds $K_4Pd(PS_4)_2$ (**I**), $Cs_4Pd(PSe_4)_2$ **(II)**, and $Cs_{10}Pd(PSe_4)_4$ **(III)** and the solid-state $KPdPS_4$ (**IV**), $K_2PdP_2S_6$ **(V)**, and $Cs_2PdP_2Se_6$ **(VI)**. Compounds **I**−**III** are air and water sensitive, while **IV**−**VI** are air and water stable. All crystals are red or dark red except those of **VI**, which are black. All of them exhibit a rodlike shape. Compound **I** crystallizes in the triclinic space group $P\bar{1}$ (No. 2) with a = 6.380(1) Å, b = 6.897(1) Å, c = 8.999(1) Å, α = 87.777(8)°, β = 81.581(8)°, γ = 84.429(9)°, and Z = 1. Compound **II** crystallizes in the monoclinic space group $P2_1/c$ (No. 14) with a = 7.491(2) Å, b = 13.340(2) Å, c = 10.030(3) Å, β = 92.21(2)°, and Z = 2. Compound **III** crystallizes in the tetragonal space group $P\bar{4}2c$ (No. 112) with $a = b$ = 13.949(2) Å, c = 11.527(2) Å, and Z = 4. Compound **IV** crystallizes in the tetragonal space group $P4_2/mnm$ (No. 136) with $a = b$ = 8.5337(2) Å, c = 10.5595(5) Å, and Z = 4. Compound **V** crystallizes in the orthorombic space group *Pnma* (No. 62) with a = 15.612(2) Å, b = 7.0724(7) Å, c = 10.080(1) Å, and Z = 4. Compound **VI** crystallizes in the monoclinic space group $C2/c$ (No. 15) with a = 12.9750(4) Å, b = 8.3282(2) Å, c = 13.0568(1) Å, β = 102.940(2)°, and Z = 4. Compounds **I**−**III** contain the discrete complexes $[Pd(PQ_4)_2]^{4-}$ (Q = S, Se). The mixed salt **III** contains additional noncoordinating $[PSe_4]^{3-}$ units. The structure of **IV** consists of Pd(II) in square planar sulfur coordination linked by edge-sharing $[PS_4]^{3-}$ tetrahedral groups to produce one-dimensional chains. The structures of **V** and **VI** feature the $[P_2Q_6]^{4-}$ (Q = S, Se) group coordinated to the square planar Pd^{2+} atoms, yielding $[PdP_2Q_6]_n^{2n-}$ chains. Physical characterization was performed with DTA, far-IR spectroscopy, solid-state UV/vis diffuse reflectance spectroscopy, and single-crystal optical transmission.

Introduction

The polychalcophosphate flux method is very powerful in accessing complex thiophosphate and selenophosphate compounds.[1] The first compounds reported from an $A_xP_yS_z$ flux reaction were $ABiP_2S_7$ (A = K, Rb).[2] Further explorations in these fluxes yielded several unusual compounds such as $A_3M(PS_4)_2$ (A = Rb, Cs; M = Sb, Bi),[3] $Cs_3Bi_2(PS_4)_3$,[3] $Na_{0.16}Bi_{1.28}P_2S_6$,[3] $A_2MP_2Se_6$ (A = K, Rb; M = Mn, Fe),[1] $A_2M_2P_2Se_6$ (A = K, Cs; M = Cu, Ag),[1] KMP_2Se_6 (M = Sb, Bi),[4] $Cs_8M_4(P_2Se_6)_5$ (M = Sb, Bi),[5] $APbPSe_4$,[6] $A_4M(PSe_4)_2$ (A = Rb, Cs; M = Pb, Eu),[6] $Rb_4Ti_2(P_2Se_9)_2(P_2Se_7)$,[7a] $KTiPSe_5$,[7a] $K_3RuP_5Se_{10}$,[7b] $A_2AuP_2Se_6$ (A = K, Rb),[8a] $A_3AuP_2Se_8$ (A = K, Rb, Cs),[8b] and $A_2Au_2P_2Se_6$ (A = K, Rb).[8b] More recently, $K_2UP_3Se_9$,[9a] $Rb_4U_4P_4Se_{26}$,[9b] and $K(RE)P_2Se_6$ (RE = Y, La, Ce, Pr, Gd)[10] were reported. This method also gives rise to molecular compounds such as $Cs_4P_2Se_9$,[7] $A_5Sn(PSe_5)_3$ (A = K, Rb),[11a] $A_6Sn_2Se_4(PSe_5)_2$ (A = Rb, Cs),[11a] and $Rb_8M_4(Se_2)_2(PSe_4)_4$ (M = Hg, Cd).[11b] Such a rich structural chemistry highlights the ability of phosphorus to adopt different chemical environments according to the nature of the metal and its coordination preference. It is noteworthy, that access to these compounds is more advantageous through the flux method than by using "wet" chemistry, since the highly charged $[P_yQ_z]^{n-}$ species are stabilized in solution with great difficulty.

The A/Pd/P/Q chemistry was investigated for mainly two reasons. First, the preference of Pd^{2+} to adopt square planar centers would most probably result in new structural types, and second, the known Pd/P/Q ternary compounds not only depart from the very stable and well-known MPQ_3 structure type, but they also possess interesting properties. One of them, the layered $Pd_3(PS_4)_2$,[12] has been studied as a possible semiconductor electrode with built-in catalytic properties.[13] Moreover, the

[⊗] Abstract published in *Advance ACS Abstracts,* November 15, 1997.

(1) (a) McCarthy, T. J.; Kanatzidis, M. G. *Inorg. Chem.* **1995**, *34*, 1257 and references therein. (b) Sutorik, A.; Kanatzidis, M. G. *Prog. Inorg. Chem.* **1995**, *43*, 151.
(2) McCarthy, T. J.; Hogan, T.; Kannewurf, C. R; Kanatzidis, M. G. *Chem. Mater.* **1994**, *6*, 1072.
(3) McCarthy, T. J.; Kanatzidis, M. G. *J. Alloys Compd.* **1996**, *236*, 70.
(4) McCarthy, T. J.; Kanatzidis, M. G. *J. Chem. Soc., Chem. Commun.* **1994**, 1089.
(5) McCarthy, T. J.; Kanatzidis, M. G. *Chem. Mater.* **1993**, *5*, 1061.
(6) Chondroudis, K.; McCarthy, T. J.; Kanatzidis, M. G. *Inorg. Chem.* **1996**, *35*, 840.
(7) (a) Chondroudis, K.; Kanatzidis, M. G. *Inorg. Chem.* **1995**, *34*, 5401. (b) Chondroudis, K.; Kanatzidis, M. G. *Angew. Chem., Int. Ed. Engl.* **1997**, *36*, 1324.
(8) (a) Chondroudis, K.; McCarthy, T. J.; Kanatzidis, M. G. *Inorg. Chem.* **1996**, *35*, 3451. (b) Chondroudis, K.; Hanko, A. J.; Kanatzidis, M. G. *Inorg. Chem.* **1997**, *36*, 2623.
(9) (a) Chondroudis, K.; Kanatzidis, M. G. *C. R. Acad. Sci. Paris, Ser. B* **1996**, *322*, 887. (b) Chondroudis, K.; Kanatzidis, M. G. *J. Am. Chem. Soc.* **1997**, *119*, 2574.
(10) (a) Chen, J. H.; Dorhout, P. K. *Inorg. Chem.* **1995**, *34*, 5705. (b) Chen, J. H.; Dorhout, P. K.; Ostenson, J. E. *Inorg. Chem.* **1996**, *35*, 5627.
(11) (a) Chondroudis, K.; Kanatzidis, M. G. *J. Chem. Soc., Chem. Commun.* **1996**, 1371. (b) Chondroudis, K.; Kanatzidis, M. G. *J. Chem. Soc., Chem. Commun.* **1997**, 401.

S0020-1669(97)00593-4 CCC: $14.00

PdPSe[12] was found to be photoactive material with high quantum efficiencies below 800 nm, and it was suggested that it might be useful in photocatalytic reactions.[14]

In addition, ternary and quaternary metal chalcogenides containing an alkali metal are often characterized by highly anisotropic, low-dimensional structures because of the ionic character of the 1A element−chalcogen bonds and the covalent character of the bonds between Pd (and P) and Q atoms.[15] An interesting process with these types of compounds is the ion exchange of the alkali metal ions with large organic cations in polar solutions. Such a substitution can be topotactic, or it can induce unusual structural rearrangements and the stabilization of new complexes.[16]

In this work, we examine the reactivity of Pd in polychalcophosphate fluxes and we report the synthesis, the structure, and the optical and thermal properties of the new quaternary compounds $K_4Pd(PS_4)_2$, $Cs_4Pd(PSe_4)_2$, $Cs_{10}Pd(PSe_4)_4$, $KPdPS_4$, $K_2PdP_2S_6$, and $Cs_2PdP_2Se_6$. The first three contain the discrete $[Pd(PQ_4)_2]^{4-}$ (Q = S, Se) complexes, while the latter three contain infinite one-dimensional anions. $Cs_{10}Pd(PSe_4)_4$ was used as a starting material to form $Cs_2PdP_2Se_6$.

Experimental Section

1. Reagents. The reagents mentioned in this study were used as obtained unless noted otherwise: (i) Pd metal (99.99%), Johnson Matthey/AESAR Group, Seabrook, NH; (ii) phosphorus pentasulfide (P_2S_5), 99.999% purity, Aldrich Chemical Co., Milwaukee, WI; (iii) red phosphorus powder, −100 mesh, Morton Thiokol, Inc., Danvers, MA. (iv) cesium metal, analytical reagent, Johnson Matthey/AESAR Group, Seabrook, NH; (v) potassium metal, analytical reagent, Aldrich Chemical Co., Milwaukee, WI; (vi) sulfur powder, sublimed, J. T. Baker Chemical Co., Phillipsburg, NJ; (vii) selenium powder, 99.5+% purity, −100 mesh, Aldrich Chemical Co., Inc., Milwaukee, WI; (viii) *N*,*N*-dimethylformamide (DMF), reagent grade, EM Science, Inc., Gibbstown, NJ; (ix) diethyl ether, ACS anhydrous, EM Science, Inc., Gibbstown, NJ; (x) methanol (MeOH), ACS anhydrous, EM Science, Inc., Gibbstown, NJ.

2. Syntheses. Yields are calculated on the basis of the theoretical weight of the compound by assuming that all of the metal reacts quantitatively.

Cs_2Se and **K_2S_3** were prepared by reacting stoichiometric amounts of the elements in liquid ammonia as described elsewhere.[1]

Preparation of $K_4Pd(PS_4)_2$ (I). A mixture of Pd (0.30 mmol), P_2S_5 (0.3 mmol), and K_2S_3 (0.6 mmol) was sealed under vacuum in a silica tube and slowly heated (5 °C·h^{-1}) to 650 °C for 10 d, followed by cooling to room temperature at 10 °C·h^{-1}. The excess flux was removed with DMF to reveal red crystals (75% yield based on Pd). The crystals disintegrate in water and over a long exposure to air. For this reason, the crystals were kept under nitrogen. Microprobe analysis with a scanning electron microscope (SEM) gave an average composition of $K_{3.7}PdP_{1.9}S_{7.7}$.

Preparation of $Cs_4Pd(PSe_4)_2$ (II). A mixture of Pd (0.30 mmol), P_2Se_5 (0.45 mmol), Cs_2Se (0.90 mmol), and Se (2.40 mmol) was sealed under vacuum in a Pyrex tube and heated to 495 °C for 4 d followed by cooling to 150 °C at 2 °C·h^{-1}. The excess $Cs_xP_ySe_z$ flux was removed with DMF to reveal dark red rodlike crystals and traces of black plates of PdSe that were subsequently manually removed (72% yield based on Pd). The crystals disintegrate in water and over a long exposure to air. Microprobe analysis performed on a large number of single crystals gave an average composition of $Cs_{3.8}PdP_{2.1}Se_{7.7}$.

Preparation of $Cs_{10}Pd(PSe_4)_4$ (III). A mixture of Pd (0.30 mmol), P_2Se_5 (0.45 mmol), Cs_2Se (1.20 mmol), and Se (2.40 mmol) was sealed under vacuum in a Pyrex tube and heated to 490 °C for 3 d followed by cooling to 150 °C at 3 °C·h^{-1}. The excess $Cs_xP_ySe_z$ flux was removed with DMF to reveal a mixture of red rodlike crystals (90%) of $Cs_{10}Pd(PSe_4)_4$ and dark red rods of $Cs_4Pd(PSe_4)_2$ (10%). The crystals disintegrate in water and over a long exposure to air. Microprobe analysis gave an average composition of $Cs_{9.7}PdP_{4.2}Se_{15.7}$.

Preparation of $KPdPS_4$ (IV). A mixture of Pd (0.30 mmol), P_2S_5 (0.15 mmol), and K_2S_3 (0.15 mmol) was sealed under vaccum in a silica tube and slowly heated (5 °C·h^{-1}) to 650 °C for 10 d, followed by cooling to room temperature at 10 °C·h^{-1}. The excess flux was removed with water to reveal dark red crystals (68% yield based on Pd). The crystals are air and water stable. Microprobe analysis gave an average composition of $K_{1.0}PdP_{0.9}S_{3.9}$.

Preparation of $K_2PdP_2S_6$ (V). **V** was initially obtained as a byproduct of the successful synthesis of $KNi_xPd_{1-x}PS_4$ ($x = 0.4$) solid solution from a mixture of Pd (0.15 mmol), Ni (0.15 mmol), P_2S_5 (0.15 mmol), and K_2S_3 (0.15 mmol). The synthesis conditions were similar to those for $KPdPS_4$ **(IV)**. Only one crystal was obtained. Up to now, attempts to prepare **V** in great amounts without any trace of Ni failed.

Preparation of $Cs_2PdP_2Se_6$ (VI). Method A. A mixture of Pd (0.25 mmol), P_2Se_5 (0.50 mmol), Cs_2Se (0.75 mmol), and Se (2.50 mmol) was sealed under vacuum in a Pyrex tube and heated to 490 °C for 4 d, followed by cooling to 150 °C at 2 °C·h^{-1}. Most of the excess $Cs_xP_ySe_z$ flux was removed with degassed DMF. Following that, the product was washed with ∼2 mL of tri-*n*-butylphosphine to remove residual elemental Se. Further washing with anydrous ether revealed black, irregular, rodlike crystals (∼60%) and residual flux in a form of a gray powder (∼40%).

Method B. Pure material was obtained from a mixture of $Cs_{10}Pd(PSe_4)_4$ (0.2 mmol), Pd (0.8 mmol), P (1.2 mmol), and Se (2.8 mmol) that was sealed under vacuum in a Pyrex tube and heated to 480 °C for 4 d, followed by cooling to 150 °C at 2 °C·h^{-1}. Washings with DMF, tri-*n*-butylphosphine, and ether revealed analytically pure crystals of **VI**. The crystals are air and water stable. Microprobe analysis with a scanning electron microscope (SEM), performed on a large number of single crystals, gave an average composition of $Cs_{1.8}PdP_{2.0}Se_{5.9}$.

3. Physical Measurements. (a) Powder X-ray Diffraction. Analyses of **II**, **III**, and **VI** were performed using a calibrated Rigaku-Denki/RW400F2 (Rotaflex) rotating-anode powder diffractometer controlled by an IBM computer, operating at 45 kV/100 mA and with a 1°/min scan rate, employing Ni-filtered Cu radiation. Samples were ground to a fine powder and mounted by spreading the sample onto a special etched-glass holder. Powder patterns were calculated with CERIUS^2 software.[17] Analyses of **I** and **IV** were performed on a CPS 120 INEL X-ray powder diffractometer using monochromatized radiation Cu K-L_{III} ($\lambda = 1.540\,49$ Å) and equipped with a position-sensitive detector calibrated with $Na_2Ca_3Al_{12}F_{14}$ as standard. Powder was introduced in a 0.1 mm Lindemann capillary. Calculated and observed XRD patterns are deposited in the Supporting Information. Crystal parameters of compound **V** were determined from least-squares refinement on 30 peaks on the crystal diffractometer.

(b) Infrared Spectroscopy. Infrared spectra, in the far-IR region (600−50 cm^{-1}), were recorded on a computer-controlled Nicolet 750 Magna-IR Series II spectrophotometer equipped with a TGS/PE detector and silicon beam splitter in 4 cm^{-1} resolution. The samples were ground with dry CsI into fine powders and pressed into translucent pellets.

(c) Solid State UV/Vis/Near-IR Spectroscopy. Optical diffuse reflectance measurements were performed at room temperature using a Shimadzu UV-3101PC double beam, double monochromator spectrophotometer. The instrument is equipped with integrating sphere and controlled by a personal computer. $BaSO_4$ was used as a 100% reflectance standard for all materials. Samples are prepared by grinding them to fine powders and spreading them on a compacted surface of the powdered standard material, preloaded into a sample holder. The reflectance versus wavelength data generated can be used to estimate

(12) Bither, T. A.; Donohue, P. C.; Young, H. S. *J. Solid State Chem.* **1971**, *3*, 300.
(13) Folmer, J. C. W.; Turner, J. A.; Parkinson, B. A. *J. Solid State Chem.* **1987**, *68*, 28.
(14) Marzik, J. V.; Kershaw, R.; Dwight, K.; Wold, A. *J. Solid State Chem.* **1982**, *44*, 382.
(15) Bronger, W.; Müller, P. *J. Less Common Met.* **1984**, *100*, 241.
(16) Sayettat, J.; Jobic, S.; Fourmigue, M.; Brec, R.; Batail, P. To be submitted for publication.
(17) *CERIUS^2*, Version 1.6; Molecular Simulations Inc.: Cambridge, England, 1994.

a material's band gap by converting reflectance to absorption data as described earlier.[18]

(d) Single-Crystal Optical Transmission. Room-temperature single-crystal optical transmission spectra were obtained on a Hitachi U-6000 microscopic FT spectrophotometer mounted on an Olympus BH2-UMA metallurgical microscope over a range of 380−900 nm. Crystals lying on a glass slide were positioned over the light source, and the transmitted light was detected from above.

(e) Differential Thermal Analysis (DTA). DTA experiments were performed on a computer-controlled Shimadzu DTA-50 thermal analyzer. Typically a sample (~25 mg) of ground crystalline material was sealed in a quartz ampule under vacuum. A quartz ampule of equal mass filled with Al_2O_3 was sealed and placed on the reference side of the detector. The sample was heated to the desired temperature at 10 °C/min, then isothermed for 10 min, and finally cooled to 50 °C at the same rate. Residue of the DTA experiment was examined by X-ray powder diffraction. To evaluate congruent melting, we compared the X-ray powder diffraction patterns before and after the DTA experiments, as well as monitored the stability/reproducibility of the DTA diagrams upon cycling the above conditions at least two times.

(f) Semiquantitative Microprobe Analyses. The analyses were performed using a JEOL JSM-6400V scanning electron microscope (SEM) equipped with a TN 5500 EDS detector. Data acquisition was performed with an accelerating voltage of 20 kV and 30 s accumulation time.

(g) Single-Crystal X-ray Crystallography. The single-crystal data collections were made on a Siemens P4 diffractometer (Ag K-$L_{2,3}$ radiation and graphite monochromator) for compounds **I** and **IV** and on an Enraf-Nonius CAD4-F diffractometer (Mo K-$L_{2,3}$ radiation and graphite monochromator) for **V**. Intensity data for **II** and **III** were collected using a Rigaku AFC6S four-circle automated diffractometer equipped with a graphite crystal monochromator. An $\omega-2\theta$ scan mode was used. Crystal stability was monitored with three standard reflections whose intensities were checked every 150 reflections, and unless noted, no crystal decay was detected in any of the compounds. A Siemens SMART Platform CCD diffractometer was used to collect data from a crystal of **VI**. An empirical absorption correction[19a] was applied to the data. The space groups were determined from systematic absences and intensity statistics. Owing to the small size of the crystals of **I**, **IV**, and **V** and their low linear absorption coefficient, no absorption correction was applied to them. An empirical absorption correction based on ψ scans was applied to all data for compounds **II** and **III**, followed by a DIFABS correction after full isotropic refinement and before a full anisotropic refinement as recommended.[19b] The structures were solved by direct methods using SHELXS-86 software[20a] (for all compounds), and full-matrix least-squares refinement was performed using the TEXSAN software package[20b] or the SDS program.[21] The presence of a structural disorder in **VI**, along with the relatively high thermal parameters of the atoms, prompted us to search for a superstructure. Investigations with long-frame data collection on a SMART CCD diffractometer and by long-exposure axial photographs on a Rigaku AFC6S four-circle diffractometer did not reveal any superstructure reflections. For **I**, data were collected for $-10 < h < 10$, $-11 < k < 11$, $-14 < l < 14$ with $F_o^2 > 3\sigma(F_o^2) = 1541$. For **II**, data were collected for $0 < h < 9$, $0 < k < 16$, $-12 < l < 12$ with $F_o^2 > 3\sigma(F_o^2) = 1391$. For **III**, data were collected for $0 < h < 17$, $0 < k < 17$, $0 < l < 14$ with $F_o^2 > 3\sigma(F_o^2) = 830$. For **IV**, data were collected for $-1 < h < 15$, $-1 < k < 15$, $-1 < l < 18$ with $F_o^2 > 3\sigma(F_o^2) = 430$. For **V**, data were collected for $-11 < h < 11$, $-3 < k < 25$, $-3 < l < 16$ with $F_o^2 > 3\sigma(F_o^2) = 741$. For **VI**, data were collected for $0 < h < 14$, $-9 < k < 9$, $-14 < l < 14$ with $F_o^2 > 3\sigma(F_o^2) = 650$. The complete data collection parameters and details of the structure solution and refinement are given in Table 1. The coordinates of all atoms, average temperature factors, and their estimated standard deviations are given in Tables 2−7.

Table 1. Crystallographic data for **I**−**IV**

	$K_4Pd(PS_4)_2$[a]	$Cs_4Pd(PSe_4)_2$	$Cs_{10}Pd(PSe_4)_4$
fw	581.18	1331.65	2822.70
a, Å	6.380(1)	7.491(2)	13.949(2)
b, Å	6.897(1)	13.340(2)	13.949(2)
c, Å	8.999(2)	10.030(3)	11.527(2)
α, deg	87.777(8)	90.00	90.00
β, deg	81.581(8)	92.21(2)	90.00
γ, deg	84.429(9)	90.00	90.00
Z; *V*, Å^3	1; 389.8(2)	2; 1001.6(4)	2; 2242.7(6)
λ, Å	0.560 86	0.710 69	0.710 69
space group	*P*$\bar{1}$ (No. 2)	$P2_1/c$ (No. 14)	$P\bar{4}2c$ (No. 112)
D_{calc}, g/cm^3	2.469	4.415	4.180
μ, cm^{-1}	17.8	225.64	213.61
temp, °C	23	−100	23
final R/R_w,[b] %	3.9/5.0	2.9/3.8	3.8/4.3

	$KPdPS_4$[a]	$K_2PdP_2S_6$	$Cs_2PdP_2Se_6$
fw	304.5	438.9	907.92
a, Å	8.5337(2)	15.612(2)	12.9750(4)
b, Å	8.5337(2)	7.0724(7)	8.3282(2)
c, Å	10.5595(5)	10.080(1)	13.0568(1)
α, deg	90.0	90.0	90.0
β, deg	90.0	90.0	102.940(2)
γ, deg	90.0	90.0	90.0
Z; *V*, Å^3	4; 769.0(1)	4; 1113.0(2)	4; 1375.07(5)
λ, Å	0.560 86	0.710 69	0.710 73
space group	$P4_2/mnm$ (No. 136)	*Pnma* (No. 62)	*C*2/*c* (No. 15)
D_{calc}, g/cm^3	2.631	2.619	4.385
μ, cm^{-1}	21.4	30.7	226.37
temp, °C	23	23	−141
final R/R_w,[b] %	2.5/3.0	4.8/5.4	6.7/7.5

[a] Refined cell parameters were obtained from the X-ray powder diagram. [b] $R = \sum(|F_o| - |F_c|)/\sum|F_o|$. $R_w = [\sum w(|F_o| - |F_c|)^2/\sum w|F_o|^2)^{1/2}$.

Table 2. Positional Parameters and B_{eq} for $K_4Pd(PS_4)_2$

atom	*x*	*y*	*z*	B_{eq},[a] Å^2
Pd	0	0	0	1.43(2)
S(1)	0.2235(3)	0.5249(2)	−0.1850(2)	2.23(4)
S(2)	−0.3268(2)	−0.0405(2)	0.1496(2)	1.96(3)
S(3)	−0.1353(2)	0.1953(2)	−0.1884(2)	1.78(3)
S(4)	0.2410(3)	0.2541(2)	−0.4878(2)	2.39(4)
P	0.1728(2)	0.2672(2)	−0.2628(2)	1.48(3)
K(1)	0.2926(2)	0.3343(2)	0.1409(2)	2.69(3)
K(2)	0.2553(2)	0.7788(2)	−0.4775(2)	3.00(4)

[a] *B* values for anisotropically refined atoms are given in the form of the isotropic equivalent displacement parameter defined as $B_{eq} = (4/3)[a^2B(1,1) + b^2B(2,2) + c^2B(3,3) + ab(\cos\gamma)B(1,2) + ac(\cos\beta)B(1,3) + bc(\cos\alpha)B(2,3)$.

Table 3. Positional Parameters and B_{eq} Values for $Cs_4Pd(PSe_4)_2$

atom	*x*	*y*	*z*	B_{eq},[a] Å^2
Cs(1)	0.2326(1)	0.84222(5)	0.03406(7)	1.22(3)
Cs(2)	0.6831(1)	0.63163(5)	0.18218(7)	1.13(3)
Pd	1	$^1/_2$	0	0.67(4)
Se(1)	−0.2611(2)	0.89286(8)	0.0455(1)	1.11(4)
Se(2)	0.1908(1)	0.57571(8)	0.1776(1)	0.85(4)
Se(3)	−0.0233(1)	0.65041(8)	−0.1390(1)	1.02(4)
Se(4)	−0.5118(1)	0.87186(8)	0.3412(1)	1.06(4)
P	−0.2626(4)	0.9192(2)	0.2576(3)	0.6(1)

[a] *B* values for anisotropically refined atoms are given in the form of the isotropic equivalent displacement parameter defined as $B_{eq} = (4/3)[a^2B(1,1) + b^2B(2,2) + c^2B(3,3) + ab(\cos\gamma)B(1,2) + ac(\cos\beta)B(1,3) + bc(\cos\alpha)B(2,3)$.

Results and Discussion

1. Description of Structures. (a) Compounds with the $[Pd(PQ_4)_2]^{4-}$ Anion. $K_4Pd(PS_4)_2$ **(I)** and $Cs_4Pd(PSe_4)_2$ **(II)**

(18) McCarthy, T. J.; Ngeyi, S.-P.; Liao J.-H.; DeGroot, D.; Hogan, T.; Kannewurf, C. R.; Kanatzidis, M. G. *Chem. Mater.* **1993**, *5*, 331.
(19) (a) Blessing, R. H. *Acta Crystallogr.* **1995**, *A51*, 33. (b)Walker, N.; Stuart, D. *Acta Crystallogr.* **1983**, *A39*, 158.
(20) (a) Sheldrick, G. M. In *Crystallographic Computing 3*; Sheldrick, G. M., Kruger, C., Doddard, R., Eds.; Oxford University Press: Oxford, England, 1985; p 175. (b) Gilmore G. J. *Appl. Crystallogr.* **1984**, *17*, 42.
(21) Petricek, V. SDS95. Institute of Physics, Praha, Czech Republic, 1995.

Table 4. Positional Parameters and B_{eq} Values for $Cs_{10}Pd(PSe_4)_4$

atom	*x*	*y*	*z*	B_{eq},[a] Å^2
Cs(1)	0.3483(1)	1/2	1/4	2.78(9)
Cs(2)	1/2	0	0.0456(2)	3.4(1)
Cs(3)	0.2564(4)	0.2552(3)	−0.0036(4)	2.4(1)
Cs(4)	0.1620(1)	0	1/4	2.79(8)
Pd(1)	0	1/2	1/4	1.41(6)
Se(1)	0.1184(1)	0.3709(1)	0.2449(8)	1.98(9)
Se(2)	0.0005(7)	0.1747(2)	0.0946(2)	2.48(9)
Se(3)	0.3705(1)	0.1488(1)	0.2534(7)	2.23(9)
Se(4)	0.5019(7)	0.3298(1)	0.0926(2)	2.07(8)
P(1)	0	0.2606(4)	1/4	1.4(3)
P(2)	1/2	0.2407(5)	1/4	1.4(3)

[a] *B* values for anisotropically refined atoms are given in the form of the isotropic equivalent displacement parameter defined as $B_{eq} = (4/3)[a^2B(1,1) + b^2B(2,2) + c^2B(3,3) + ab(\cos\gamma)B(1,2) + ac(\cos\beta)B(1,3) + bc(\cos\alpha)B(2,3)$.

Table 5. Positional Parameters and B_{eq} Values for $KPdPS_4$

atom	*x*	*y*	*z*	B_{eq},[a] Å^2
Pd(1)	0	0	0	2.05(2)
Pd(2)	0	0	0.5	2.25(2)
S(1)	−0.14256(8)	0.14256	0.64930(10)	3.01(2)
S(2)	−0.2719(1)	−0.0124(1)	0	2.69(2)
P	−0.2494(1)	0.2494	0.5	2.38(2)
K	0	0.5	0.25	3.75(3)

[a] *B* values for anisotropically refined atoms are given in the form of the isotropic equivalent displacement parameter defined as $B_{eq} = (4/3)[a^2B(1,1) + b^2B(2,2) + c^2B(3,3) + ab(\cos\gamma)B(1,2) + ac(\cos\beta)B(1,3) + bc(\cos\alpha)B(2,3)$.

Table 6. Positional Parameters and B_{eq} Values for $K_2PdP_2S_6$

atom	*x*	*y*	*z*	B_{eq},[a] Å^2
Pd	1/2	1/2	1/2	1.29(2)
S(1)	0.4909(3)	0.5107(7)	0.7303(3)	1.82(1)
S(2)	0.2665(2)	0.4886(8)	0.3330(4)	2.44(1)
S(3)	0.4041(3)	1/4	0.5278(5)	1.34(1)
S(4)	0.5911(4)	3/4	0.9698(5)	2.13(2)
P(1)	0.5569(3)	3/4	0.7829(6)	1.26(1)
P(2)	0.3316(3)	1/4	0.3513(6)	1.18(1)
K(1)	0.6833(3)	1/4	0.4141(5)	2.29(2)
K(2)	0.6194(4)	1/4	0.9359(7)	3.63(2)

[a] *B* values for anisotropically refined atoms are given in the form of the isotropic equivalent displacement parameter defined as $B_{eq} = (4/3)[a^2B(1,1) + b^2B(2,2) + c^2B(3,3) + ab(\cos\gamma)B(1,2) + ac(\cos\beta)B(1,3) + bc(\cos\alpha)B(2,3)$.

Table 7. Positional Parameters and B_{eq} Values for $Cs_2PdP_2Se_6$

atom	*x*	*y*	*z*	B_{eq},[a] Å^2
Cs	0.8679(1)	0.1740(2)	0.3662(1)	4.32(5)
Pd	1.0000	−0.5000	0.5000	5.02(8)
Se(1)	0.8888(2)	−0.4697(3)	0.6276(2)	4.32(7)
Se(2)	1.1278(2)	−0.0682(3)	0.3596(2)	3.95(7)
Se(3)	0.8763(2)	−0.3134(4)	0.3882(2)	4.58(7)
P(1)[b]	0.912(2)	−0.293(3)	0.226(2)	3.7(6)
P(2)[b]	1.031(2)	−0.289(3)	0.338(2)	3.7(7)
P(3)[b]	1.028(2)	0.404(3)	0.715(2)	2.5(6)
P(4)[b]	1.026(2)	−0.182(3)	0.226(2)	2.5(6)

[a] *B* values for anisotropically refined atoms are given in the form of the isotropic equivalent displacement parameter defined as $B_{eq} = (4/3)[a^2B(1,1) + b^2B(2,2) + c^2B(3,3) + ab(\cos\gamma)B(1,2) + ac(\cos\beta)B(1,3) + bc(\cos\alpha)B(2,3)$. [b] The occupancy factor of this atom is 0.25 out of a maximum possible 1.00.

have discrete $[Pd(PQ_4)_2]^{4-}$ anions with the molecular structure shown in Figure 1. The $[Pd(PQ_4)_2]^{4-}$ complex consists of two $[PQ_4]^{3-}$ ligands and one Pd^{2+} center which is situated at a crystallographic center of symmetry. Each $[PQ_4]^{3-}$ tetrahedron behaves as a bidentate ligand, and two of them complete the square planar coordination of Pd^{2+}. This is reminiscent of the dithiophosphato complexes of Pd^{2+}, like $Pd[(Pr^i_2O)_2PS_2]_2$[22] and

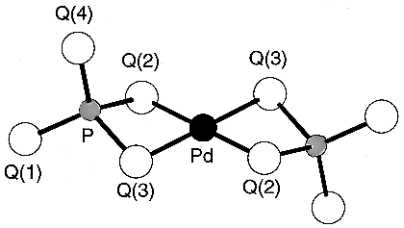

Figure 1. Structure and labeling of the discrete $[Pd(PQ_4)_2]^{4-}$ complexes in $K_4Pd(PS_4)_2$ and $Cs_4Pd(PSe_4)_2$.

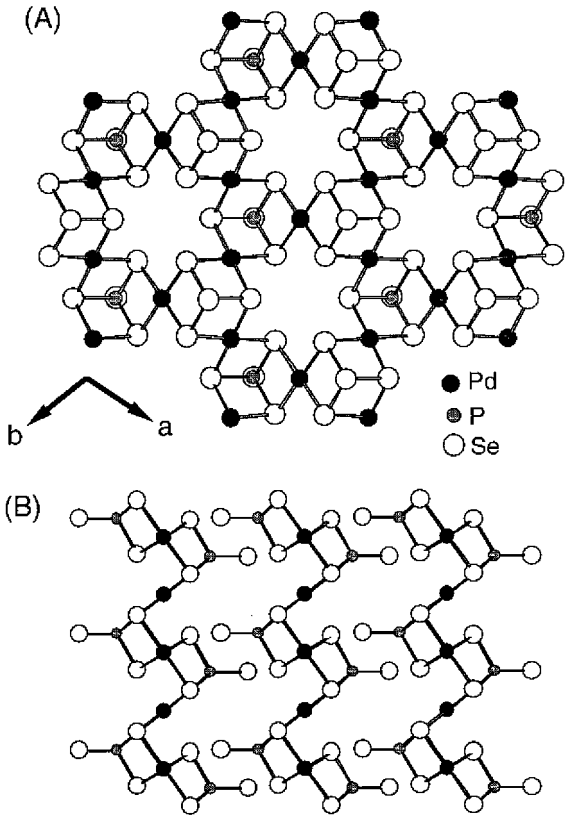

Figure 2. (A) Structure of $[Pd_3(PS_4)_2]$ viewed down the *c* axis. (B) Structure of $[Pd_3(PS_4)_2]$ viewed down the [220] direction.

$Pd[(C_8H_9O)_2PS_2]_2$,[23] in which two bidentate $[(RO)_2PS_2]^-$ ligands coordinate to square planar Pd^{2+} centers. It is also reminiscent of the tetrathiomolybdate and tetrathiotungstate complexes $(R_4N)_2Pd(MoS_4)_2$[24a] and $(R_4N)_2Pd(WS_4)_2$.[24b] The $[Pd(PQ_4)_2]^{4-}$ structure can be related to that of $Pd_3(PS_4)_2$[12] (see Figure 2). The latter has Pd^{2+} coordinated in a square planar fashion by two $[PS_4]^{3-}$ tetrahedra with the difference that every $[PS_4]^{3-}$ is triply bridging two more Pd centers. This arrangement results in an infinite two-dimensional structure. In this way $[Pd(PQ_4)_2]^{4-}$ can be regarded as a building block of $Pd_3(PS_4)_2$. PdPSe[12] bears no resemblance to our compounds, since it has a layered structure with $[PSe]^{2-}$ anions and weak Pd−Pd interactions.

The Pd−S and Pd−Se distances average at 2.340(1) and 2.451(1) Å, respectively, in **I** and **II**. There is a strong square to rectangular distortion of the Pd environment with 3.101(2) and 3.284(2) Å Q−Q distances (respectively S and Se) against 3.507(2) and 3.640(2) Å. Such a distortion originates from the

(22) Yordanov, N. D.; Ivanova, M.; Gochev, G.; Macicek, J. *Polyhedron* **1993**, *12*, 117.
(23) Roques, P. R.; Blonski, C.; Klaébé, A.; Périé, J.; Declercq, J. P.; Germain, G. *Acta Crystallogr.* **1981**, *B37*, 1756.
(24) (a) Callahan, K. P.; Piliero, P. A. *J. Chem. Soc., Chem. Commun.* **1979**, 13. (b) Callahan, K. P.; Piliero, P. A. *Inorg. Chem.* **1980**, *19*, 2619.

Table 8. Selected Distances (Å) and Angles (deg) for $K_4Pd(PS_4)_2$[a]

		Square Environment of Pd			
Pd−S(2)	2.345(1) (×2)	S(2)−S(3)	3.101(2) (×2)	S(2)−Pd−S(2)	180.00
Pd−S(3)	2.336(1) (×2)	S(2)−S(3)	3.507(2) (×2)	S(3)−Pd−S(3)	180.00
				S(3)−Pd−S(2)	97.08(5) (×2)
				S(2)−Pd−S(3)	82.92(5) (×2)
		Tetrahedral Environment of P			
P−S(1)	2.007(2)	S(1)−S(2)	3.354(2)	S(1)−P−S(2)	110.38(10)
P−S(2)	2.077(2)	S(1)−S(3)	3.383(2)	S(1)−P−S(3)	111.63(8)
P−S(3)	2.083(2)	S(1)−S(4)	3.345(2)	S(1)−P−S(4)	112.70(9)
P−S(4)	2.013(2)	S(2)−S(3)	3.101(2)	S(2)−P−S(3)	96.35(8)
		S(2)−S(4)	3.423(2)	S(2)−P−S(4)	113.63(9)
		S(3)−S(4)	3.378(2)	S(3)−P−S(4)	111.10(10)

[a] The estimated standard deviations in the mean bond lengths and the mean bond angles are calculated by the equation $\sigma_l = [\sum_n (l_n - l)^2/n(n-1)]^{1/2}$, where l_n is the length (or angle) of the nth bond, l the mean length (or angle), and n the number of bonds.

Table 9. Selected Distances (Å) and Angles (deg) for $Cs_4Pd(PSe_4)_2$[a]

		Square Environment of Pd			
Pd−Se(2)	2.457(1) (×2)	Se(2)−Se(3)	3.284(2) (×2)	Se(2)−Pd−Se(2)	180.00
Pd−Se(3)	2.446(1) (×2)	Se(2)−Se(3)	3.640(2) (×2)	Se(3)−Pd−Se(3)	180.00
				Se(3)−Pd−Se(2)	95.88(4) (×2)
				Se(2)−Pd−Se(3)	84.12(4) (×2)
		Tetrahedral Environment of P			
P−Se(1)	2.157(3)	Se(1)−Se(2)	3.718	Se(1)−P−Se(2)	115.3(1)
P−Se(2)	2.247(3)	Se(1)−Se(3)	3.617	Se(1)−P−Se(3)	110.8(1)
P−Se(3)	2.238(3)	Se(1)−Se(4)	3.582	Se(1)−P−Se(4)	111.8(1)
P−Se(4)	2.170(3)	Se(2)−Se(3)	3.284	Se(2)−P−Se(3)	94.2(1)
		Se(2)−Se(4)	3.639	Se(2)−P−Se(4)	110.0(1)
		Se(3)−Se(4)	3.669	Se(3)−P−Se(4)	112.7(1)

[a] The estimated standard deviations in the mean bond lengths and the mean bond angles are calculated by the equation $\sigma_l = [\sum_n (l_n - l)^2/n(n-1)]^{1/2}$, where l_n is the length (or angle) of the nth bond, l the mean length (or angle), and n the number of bonds.

repulsive force field induced by edge-sharing (PQ_4) tetrahedra.[25] The P−Q distances range from 2.007(2) to 2.083(2) Å for Q = S and from 2.157(3) to 2.247(3) Å for Q = Se with the noncoordinated terminal chalcogen [Q(1), Q(4)] lying closest to the phosphorus. Very similar distances have been observed in $Cs_3Bi(PS_4)_2$,[3] $CsPbPSe_4$,[6] and $K_4Eu(PSe_4)_2$.[6]

In both compounds, there are two crystallographically independent alkali metal cations. In **I**, K(1) is in an approximate monocapped trigonal prismatic coordination by sulfur [range of K(1)−S distances 3.239(2)−3.407(2) Å; average 3.334 Å]. It is interesting to note the occurrence of a short K−Pd contact at 3.487(1) Å capping a S_4 face. K(2) is coordinated by seven S atoms defining a monocapped octahedron with five short K−S distances (from 3.098(2) to 3.269(2) Å) and two long distances (3.625(2) and 3.634(2) Å) [range of K(2)−S distances 3.098(2)−3.634(2) Å; average 3.322 Å]. In compound **II**, Cs(1) is coordinated by nine Se atoms [range of Cs(1)−Se distances 3.586(2)−3.981(1) Å; average 3.764 Å] defining a tricapped trigonal prism (two capping perpendicular to rectangular faces; one caping perpendicular to the trigangular face). Cs(2) is coordinated by nine Se atoms, also [range of Cs(2)−Se distances 3.667(2)−4.026(1) Å; average 3.816 Å], with one Pd atom and one phosphorus atom located 3.520(1) and 3.928 Å from Cs(2), respectively. The insertion of the cation Pd^{2+} or P^{5+} into the coordination environment of the alkali metal does not imply any chemical bond but has to be viewed as the result of the more compact geometrical packing of the $[Pd(PQ_4)_2]^{4-}$ discrete molecules. Hence, despite the common Pd complex in $K_4Pd(PS_4)_2$ and $Cs_4Pd(PSe_4)_2$, the chemical environnments of K and Cs are very different. Selected distances and angles for **I** and **II** are given in Tables 8 and 9.

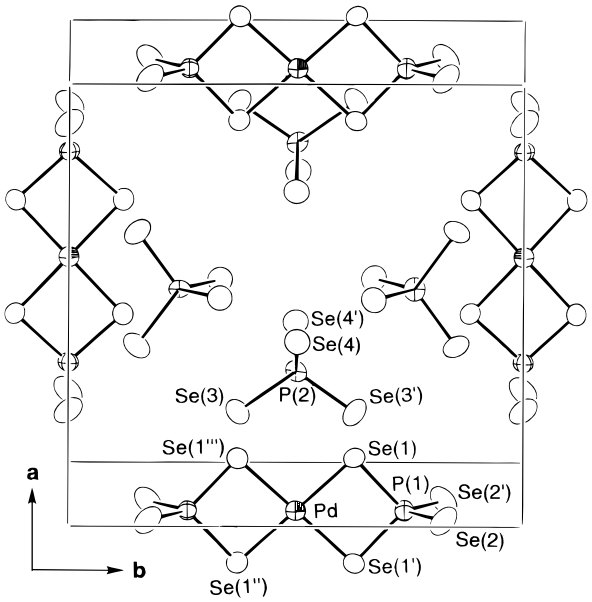

Figure 3. Structure and labeling of $Cs_{10}Pd(PSe_4)_4$ viewed down the *c* axis. Cations have been omitted for clarity.

Compound **III** is a phase that contains both discrete $[Pd(PSe_4)_2]^{4-}$ anions, which lie at a 222 crystallographic site, and uncoordinated $[PSe_4]^{3-}$ units; see Figure 3. The latter (see the P(2) group in Figure 3) is almost undisturbed by the surrounding $[Pd(PSe_4)_2]^{4-}$ anions and can be regarded almost as an ideal $[PSe_4]^{3-}$ tetrahedron. Contrasting it with the bound $[PSe_4]^{3-}$ ligand (P(1) group) reveals some interesting differences. The most apparent is the very small Se(1)−P(1)−Se(1′) angle [94.1(2)°] caused by the coordination to the Pd center. In comparison, the smaller angle for P(2) is 107.6(3)°. The degree of strain in the ligand can be expressed in terms of the *bite distance*, the separation between the two donor Se atoms. Therefore, the bite distance [Se(1)−Se(1′)] for the P(1) group

(25) (a) Gupta, N.; Seo, D. K.; Whangbo, M. H.; Jobic, S.; Rouxel, J.; Brec, R. *J. Solid State Chem.* **1997**, *128*, 181. (b) Sourisseau, C.; Cavagant, R.; Fouassier, M.; Brec, R.; Elder, S. H. *Chem. Phys.* **1995**, *195*, 351. (c) Elder, S. H.; Van der Lee, A.; Brec, R.; Canadell, E. *J. Solid State Chem.* **1995**, *116*, 107.

Table 10. Selected Distances (Å) and Angles(deg) for $Cs_{10}Pd(PSe_4)_4$[a]

		Square Environment of Pd			
Pd−Se(1)	2.444(2) (×4)	Se(1)−Se(1)	3.305(4) (×2)	Se(1)−Pd−Se(1)	85.06(9) (×2)
		Se(1)−Se(1)	3.605(4) (×2)	Se(1)−Pd−Se(1)	177.3(4) (×2)
				Se(1)−Pd−Se(1)	95.01(9) (×2)
		Tetrahedral Environment of P(1)			
P(1)−Se(1)	2.257(5) (×2)	Se(1)−Se(1)	3.305(4)	Se(1)−P(1)−Se(1)	94.1(2)
P(1)−Se(2)	2.156(4) (×2)	Se(1)−Se(2)	3.696 (×2)	Se(1)−P(1)−Se(2)	110.8(3) (×2)
		Se(1)−Se(2)	3.633 (×2)	Se(1)−P(1)−Se(2)	113.8(3) (×2)
		Se(2)−Se(2)	3.583	Se(2)−P(1)−Se(2)	112.4(3)
		Tetrahedral Environment of P(2)			
P(2)−Se(3)	2.215(4) (×2)	Se(3)−Se(3)	3.614	Se(3)−P(2)−Se(3)	109.3(3)
P(2)−Se(4)	2.198(4) (×2)	Se(3)−Se(4)	3.629 (×2)	Se(3)−P(2)−Se(4)	107.6(3) (×2)
		Se(3)−Se(4)	3.562(7) (×2)	Se(3)−P(2)−Se(4)	110.6(3) (×2)
		Se(4)−Se(4)	3.629	Se(4)−P(2)−Se(4)	111.2(3)

[a] The estimated standard deviations in the mean bond lengths and the mean bond angles are calculated by the equation $\sigma_l = [\sum_n (l_n - l)^2/n(n-1)]^{1/2}$, where l_n is the length (or angle) of the nth bond, l the mean length (or angle), and n the number of bonds.

Chart 1

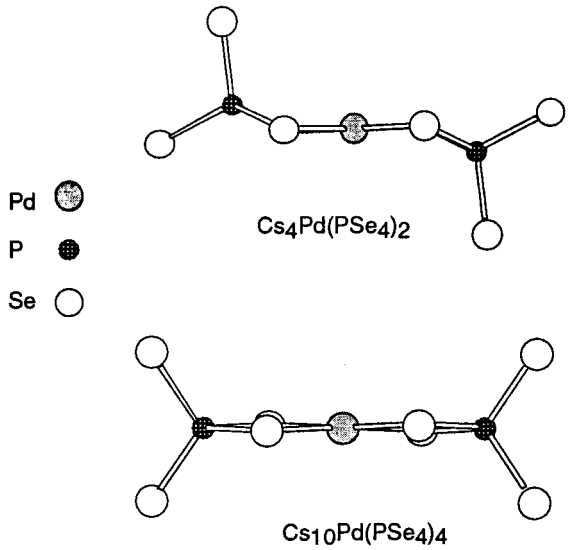

is 3.305(4) Å, whereas the smaller Se−Se distance for the P(2) group is 3.562(7) Å [Se(3)−Se(4′)]. Another distinction between the two groups is the difference between minimum and maximum P−Se distances. For the P(1) group, this difference is 0.101(5) Å (from 2.156(4) to 2.257(5) Å), and for the P(2) group, it is 0.017(4) Å (from 2.198(4) to 2.215(4) Å). The lack of homogeneity in the distances of the coordinating $[PSe_4]^{3-}$ is caused by the elongated P−Se distances of the donor Se atoms in the P(1) group.

Even though the $[Pd(PSe_4)_2]^{4-}$ anions in **II** and **III** look alike, they are conformationally different. Namely, the "rectangular" planar Pd coordination in **II** is ideal (mean deviation of Pd and Se atoms from least squares plane = 0 Å), whereas in **III** it is slightly distorted (mean deviation of Pd and Se atoms from least squares plane = 1.32 Å). In **II** the $[Pd(PSe_4)_2]^{4-}$ complex has a pseudo-chairlike conformation (the Pd−Se(2)−Se(3)−P dihedral angle is 27.4°), while in **III** the same complex is strictly planar (the corresponding Pd−Se(1)−Se(1′)−P(1) angle is 0°); see Chart 1. The Pd−Se distance in **III** is 2.444(2) Å, similar to the ones in **II**. The P−Se distances range from 2.156(4) to 2.257(5) Å with the noncoordinated selenium atoms displaying the shorter ones. Going from $Cs_4Pd(PSe_4)_2$ to $Cs_{10}Pd(PSe_4)_4$, the distortion cannot be related to an electronic effect but rather to a steric one. Hence, even if the $[Pd(PSe_4)_2]^{4-}$ and $[PSe_4]^{3-}$ entities are well separated from each other (with Se(3)−Se(1) contacts longer than 4.6 Å), the latter influences electrostatically the shape of the former through the alkaline metal ion. There are four crystallographically independent Cs cations. Cs(1) is eight-coordinated [range of Cs(1)−Se distances 3.646(6)−3.958(2) Å; average 3.740 Å]. Cs(2) is coordinated by six Se atoms [range of Cs(2)−Se distances 3.598(6)−4.146(7) Å; average 3.797 Å] and one Pd atom with a Cs(2)−Pd distance of 3.407(2) Å. Cs(3) is eight-coordinated [range of Cs(3)−Se distances 3.562(7)−3.91(1) Å; average 3.762 Å]. Cs(4) is eight-coordinated [range of Cs(4)−Se distances 3.574(2)−3.976(2) Å; average 3.775 Å]. Selected distances and angles for **III** are given in Table 10. Up to now, no sulfide analogue of **III** has been synthesized.

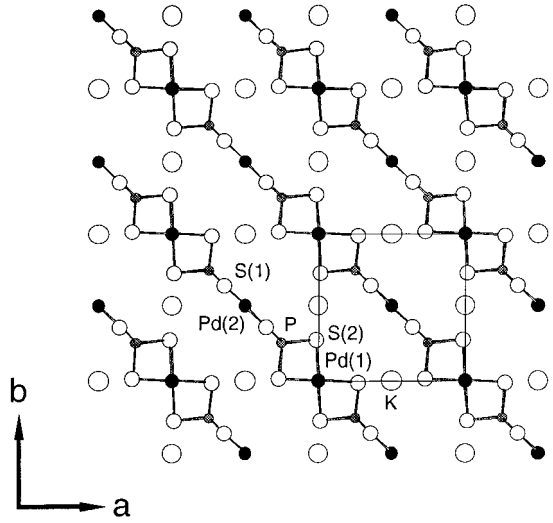

Figure 4. Structure and labeling of $KPdPS_4$.

(b) Structure of $KPdPS_4$. The structure of **IV** is one-dimensional and isomorphous with that of $KNiPS_4$.[25b,c] The infinite straight chains of $[PdPS_4]^-$ have square planar Pd^{2+} ions linked by $[PS_4]^{3-}$ ligands (see Figure 4). The chains can be thought of as made from linking terminal sulfides with Pd^{2+} ions in the $[Pd(PS_4)_2]^{4-}$ complexes. The Pd−S and P−S distances average at 2.328(1) and 2.038(1) Å, respectively. The potassium atoms are in bicapped trigonal prism coordination by sulfur and lie above and below the planes containing the $[NiPS_4]^-$ infinite chains. The average K−S distance of 3.365(1) Å is the value obtained by summing the effective ionic radii for K^+ and S^{2-}. Selected distances and angles for **IV** are given in Table 11.

(c) Structures of $K_2PdP_2S_6$ and $Cs_2PdP_2Se_6$. Both the structures of $K_2PdP_2S_6$ **(V)** and $Cs_2PdP_2Se_6$ **(VI)** are built on $[PdP_2Q_6]_n^{2n-}$ infinite chains, and they belong to the family of $A_2MP_2Q_6$ (A = K, Rb, Cs; M = Mn,[1,26] Fe,[1,26] Zn,[27] Cd,[27] Hg[27]) compounds. Remarkably, the two structures are significantly different. The $[PdP_2S_6]_n^{2n-}$ chains of **V** consist of corner-

Table 11. Selected Distances (Å) and Angles (deg) for $KPdPS_4$[a]

		Square Environment of Pd(1)			
Pd(1)−S(2)	2.323(1) (×4)	S(2)−S(2)	3.132(1) (×2)	S(2)−Pd(1)−S(2)	95.23(3) (×2)
		S(2)−S(2)	3.432(1) (×2)	S(2)−Pd(1)−S(2)	84.77(3) (×2)
				S(2)−Pd(1)−S(2)	180.00 (×2)
		Square Environment of Pd(2)			
Pd(2)−S(1)	2.333(1) (×4)	S(1)−S(1)	3.153(2) (×2)	S(1)−Pd(2)−S(1)	95.00(3) (×2)
		S(1)−S(1)	3.441(1) (×2)	S(1)−Pd(2)−S(1)	85.00(3) (×2)
				S(1)−Pd(2)−S(1)	180.00 (×2)
		Tetrahedral Environment of P			
P−S(1)	2.036(1) (×2)	S(1)−S(1)	3.153(2)	S(1)−P−S(1)	101.44(5)
P−S(2)	2.041(1) (×2)	S(1)−S(2)	3.419(1) (×4)	S(1)−P−S(2)	113.95(4) (×4)
		S(2)−S(2)	3.132(1)	S(2)−P−S(2)	100.23(6)

[a] The estimated standard deviations in the mean bond lengths and the mean bond angles are calculated by the equation $\sigma_l = [\sum_n (l_n - l)^2/n(n-1)]^{1/2}$, where l_n is the length (or angle) of the nth bond, l the mean length (or angle), and n the number of bonds.

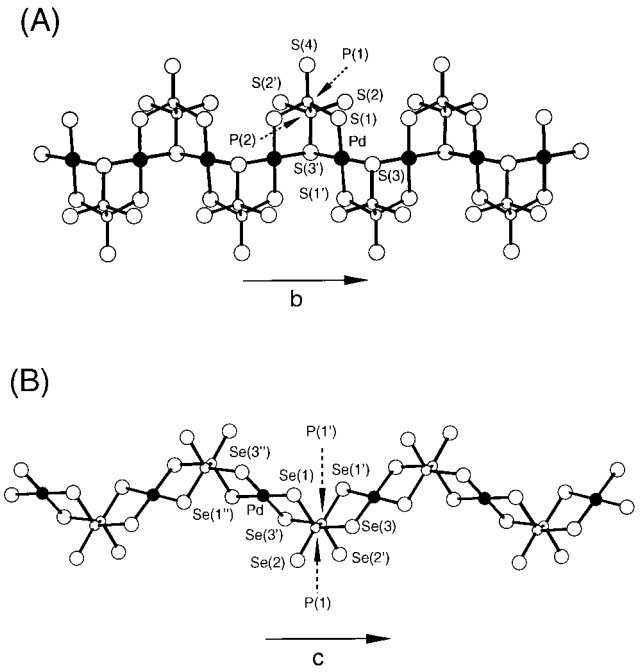

Figure 5. (A) Structure and labeling of a single $[PdP_2S_6]^{2-}$ chain viewed down the [110] crystallographic direction. (B) Structure and labeling of a single $[PdP_2Se_6]^{2-}$ chain.

sharing (PdS_4) squares defining zigzag $[PdS_3]$ infinite chains running along the *b* axis; see Figure 5A. Free S-apices of these so-defined chains are linked to the ethane-like groups which seat alternatively up and down along the chain. Hence, one phosphorus atom is bound to two successive square apices while the second P atom is linked only to the square shared corner of the chain. The $[P_2S_6]^{4-}$ group in this compound uses three of its sulfur atoms on a single P atom to bind the square planar Pd(II) atoms. The remaining three sulfur atoms on the other P atom do not participate in Pd bonding.

In sharp contast, the structure of **VI** features tetradentate $[P_2Se_6]^{4-}$ groups in which two selenium atoms from each P atom coordinate to Pd atoms, thus utilizing four out of the six possible coordination sites; see Figure 5B. Each $[P_2Se_6]^{4-}$ coordinates to two metal centers. The P−P group is positionally disordered, assuming four different orientations [P(1)−P(1′), P(2)−P(2′), P(3)−P(4)×2]; see Figure 6. Each P−P pair is oriented in such a way that there is one to one correspondence

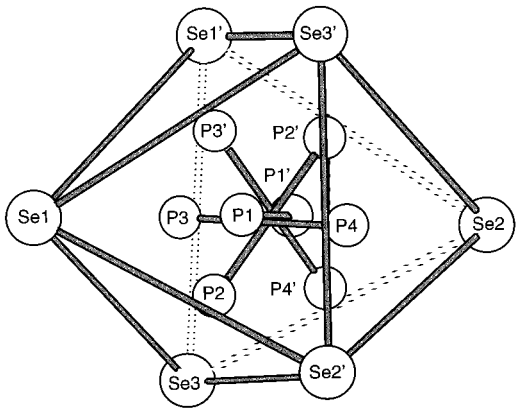

Figure 6. Disorder of the $[P_2Se_6]^{4-}$ group inside the Se octahedron. Bonds between P and Se atoms have been omitted for clarity.

between the faces of the Se octahedron and the P atoms. The $[PdP_2Se_6]_n^{2n-}$ chains propagate in the [001] direction. A key difference between **V** and **VI** is that the PdQ_4 square planes in the latter are well separated. The higher denticity of the $[P_2Se_6]^{4-}$ group in **VI** (tetradentate) satisfies four coordination sites; therefore, the PdQ_4 planes do not corner-share as observed in **V** (tridentate $[P_2S_6]^{4-}$ groups). It is tempting to attribute the different chain arrangements between **V** and **VI** to the cation size effect. The significantly smaller K^+ cations would require a higher packing of the anionic part, forcing the structure to a more compact arrangement as observed in **V**. The Pd−S distances in **V** average 2.330(3) Å, in good agreement with values calculated for **I** and **IV**. Again, we notice two types of S···S contacts inside a (PdS_4) square: S−S distances of about 3.510(6) Å between sulfur atoms belonging to a (P_2S_6) octahedron and 3.065(6) Å between sulfur atoms belonging to two different (P_2S_6) entities. The phosphorus−phosphorus distances average 2.205(8) Å, as expected. K(1) is coordinated by nine S atoms (range of K(1)−S distances 3.245(6)−3.835(3) Å; average 3.480 Å) with two Pd atoms and one P atom located at 3.474(4) and 3.538(8) Å from K(1), respectively. K(2) is also coordinated by nine S atoms (range of K(2)−S distances 3.422(8)−3.733(7) Å; average 3.583 Å). Selected distances and angles for **V** are given in Table 12. The Pd−Se distances in **VI** average 2.457(9) Å. The phosphorus−phosphorus distances average 2.21(4) Å. The $[PdP_2Se_6]_n^{2n-}$ chains are separated by nine-coordinate Cs^+ ions. Each Cs^+ cation is coordinated by six Se atoms [range of Cs−Se distances 3.583(3)−3.990(3) Å; average 3.787 Å], two P atoms [average 3.580 Å], and a Pd atom [Pd−Se 3.467(2) Å]. Selected distances and angles for **VI** are given in Table 13. The relationship of **VI** to the $A_2MP_2Se_6$ family and a more detailed structure description will be published elsewere.[27]

(26) (a) Menzel, F.; Brockner, W.; Carrillo-Cabrera, W.; von Schnering, H. G. *Z. Anorg. Allg. Chem.* **1994**, *620*, 1081. (b) Carrillo-Cabrera, W.; Sassmannhausen, J.; von Schnering, H. G.; Menzel, F.; Brockner, W. *Z. Anorg. Allg. Chem.* **1994**, *620*, 489.
(27) Chondroudis, K.; Kanatzidis, M. G. Submitted for publication.

Table 12. Selected Distances (Å) and Angles (deg) for $K_2PdP_2S_6$[a]

		Square Environment of Pd			
Pd−S(1)	2.327(3) (×2)	S(1)−S(3)	3.065(6) (×2)	S(1)−Pd−S(3)	82.0(2) (×2)
Pd−S(3)	2.333(3) (×2)	S(1)−S(3)	3.510(6) (×2)	S(1)−Pd−S(3)	97.7(2) (×2)
				S(1)−Pd−S(1)	180.00
				S(3)−Pd−S(3)	180.00
		Environment of (P_2S_6) Octahedron			
P(1)−P(2)	2.205(8)	S(1)−S(1)	3.384(7)	S(1)−P(1)−S(1)	111.2(3)
		S(1)−S(4)	3.338(6) (×2)	S(1)−P(1)−S(4)	112.7(2) (×2)
P(1)−S(1)	2.051(6) (×2)	S(2)−S(2)	3.375(8)	S(4)−P(1)−P(2)	112.0(3)
P(1)−S(4)	1.958(8)	S(2)−S(3)	3.365(6) (×2)	S(1)−P(1)−P(2)	103.8(2) (×2)
P(2)−S(2)	1.979(6) (×2)			S(2)−P(2)−S(2)	117.1(3)
P(2)−S(3)	2.110(8)			S(2)−P(2)−S(3)	110.8(2) (×2)
				S(2)−P(2)−P(1)	110.4(2) (×2)
				S(3)−P(2)−P(1)	95.4(3)

[a] The estimated standard deviations in the mean bond lengths and the mean bond angles are calculated by the equation $\sigma_l = [\sum_n (l_n - l)^2/n(n-1)]^{1/2}$, where l_n is the length (or angle) of the nth bond, l the mean length (or angle), and n the number of bonds.

Table 13. Selected Distances (Å) and Angles (deg) for $Cs_2PdP_2Se_6$[a]

		Square Environment of Pd			
Pd−Se(1)	2.449(3) (×2)	Se(1)−Se(3″)	3.357(4) (×2)	Se(1)−Pd−Se(3′)	93.81(8)
Pd−Se(3)	2.464(3) (×2)	Se(1)−Se(3′)	3.588(4) (×2)	Se(1)−Pd−Se(3″)	86.19(8)
				Se(1)−Pd−Se(1″)	180.00
		Environment of (P_2Se_6) Octahedron			
P(1)−Se(average)		2.27(4)		Pd−Se(1)−P(1)	105.2(7)
P(2)−Se(average)		2.24(3)		Pd−Se(3′)−P(1′)	110.8(6)
P(3)−Se(av)		2.23(4)			
P(4)−Se(average)		2.28(4)		Se(1)−P(1)−Se(2)	117.5(9)
				Se(1)−P(1)−Se(3)	113.7(8)
P−P (average)		2.21(4)		Se(2)−P(1)−Se(3)	117.9(9)
				Se(1)−P(1)−P(1′)	98.7(7)

[a] The estimated standard deviations in the mean bond lengths and the mean bond angles are calculated by the equation $\sigma_l = [\sum_n (l_n - l)^2/n(n-1)\}^{1/2}$, where l_n is the length (or angle) of the nth bond, l the mean length (or angle), and n the number of bonds.

2. Synthesis, Spectroscopy, and Thermal Analysis. (a) Chemical Considerations. Palladium is oxidized by polychalcogenide ions in the $A_x[P_yQ_z]$ flux forming Pd^{2+} ions which are then coordinated by the highly charged $[P_yQ_z]^{n-}$ ligands. The strongly Lewis basic conditions[1,6−9,11] used for the synthesis of **I**−**IV** stabilized the $[PQ_4]^{3-}$ ligand, which features P^{5+}. Both **II** and **III** were initially synthesized from the same reaction in a 50:50 mixture. After the structures were solved, the formulas indicated that we could exploit the difference in the Cs:Pd ratios (4:1 and 10:1, respectively) between the two compounds, in order to synthesize pure materials. Accordingly, to produce **II**, the Cs_2Se content was reduced untill PdSe started appearing as a small contaminant. For **III**, the Cs_2Se content was raised until further increase yielded $Cs_4P_2Se_9$[7a] as a contaminant. The optimum conditions yielded a mixture of 90% **III** and 10% **II** (see Synthesis).

In a recent communication we suggested the use of molecular polyselenophosphates as starting materials or building blocks for further solution- or solid-state chemistry.[11a] To examine the feasibility of this idea, we performed the reaction of eq 1

$$0.2Cs_{10}Pd(PSe_4)_4 + 0.8Pd + 1.2P + 2.8Se \xrightarrow{480\ ^\circ C} Cs_2PdP_2Se_6 \quad (1)$$

(see also Syntheses). On the basis of the stability of the $A_2MP_2Se_6$ phases,[1] we expected that $Cs_2PdP_2Se_6$ would be a stable compound. Accordingly, **III** was used as a starting material in a mixture with Pd, P, and Se in such ratios to provide a nominal composition of "$Cs_2PdP_2Se_6$". After it was heated at 480 °C, the melt was isolated to yield pure $Cs_2PdP_2Se_6$. During this redox reaction, elemental Pd^0 is being oxidized to Pd^{2+}, P^0 to P^{4+}, and Se^0 to Se^{2-}, while P^{5+} is reduced to P^{4+}. This "transformation" of a molecular to a solid-state compound suggests that new chemistry becomes available, in which one can utilize such molecular compounds as starting materials to access solid-state chalcophosphates. It becomes therefore plausible to prepare quinternary $A_xM_aM'_bP_yQ_z$ compounds according to eq 2.

$$A_xM_aP_yQ_z + M' + P + Q \rightarrow A_xM_aM'_bP_mQ_n \quad (2)$$

Scheme 1

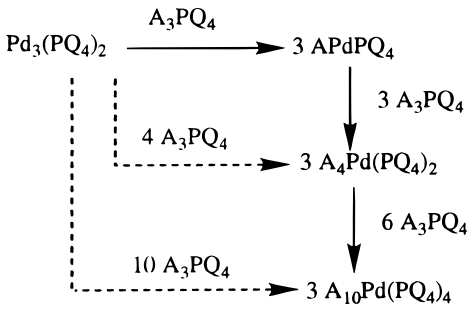

To place $KPdPS_4$, $A_4Pd(PQ_4)_2$, and $Cs_{10}Pd(PSe_4)_4$ in a greater context, it is useful to consider them as members of a series with the general formula $(A_3PQ_4)_n[Pd_3(PQ_4)_2]_m$ where ($n = 1$, $m = 1$), ($n = 4$, $m = 1$), and ($n = 10$, $m = 1$), respectively. $Pd_3(PS_4)_2$[12] would be the parent member ($n = 0$, $m = 1$) of the series. Interestingly, the Se analog $Pd_3(PSe_4)_2$ has not been reported. One can envision "dismantling" the 2-D network of $Pd_3(PQ_4)_2$ by introducing one $[PQ_4]^{3-}$ unit per formula, to obtain the 1-D chains of **IV**. To maintain electroneutrality, of course, for every $[PQ_4]^{3-}$ unit that is introduced, three A^+ cations should follow. Introduction of a further 3 equiv of $[PQ_4]^{3-}$ to **IV** results in the molecular $A_4Pd(PQ_4)_2$ phases. Finally, further "dilution" of the structure with six more $[PQ_4]^{3-}$ units forms the mixed salt **III**. This is illustrated in Scheme 1. Similar polychalcophosphate series exist for Pb[6] and Bi.[3] In the Pb case, the parent

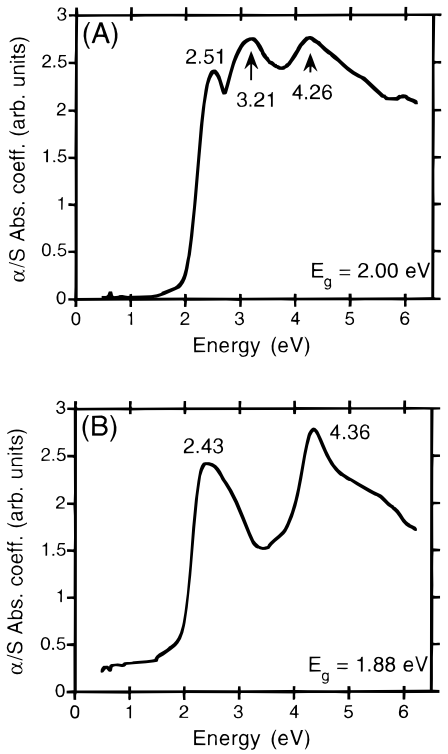

Figure 7. (A) Solid-state optical absorption spectrum for $K_4Pd(PS_4)_2$. (B) Solid-state optical absorption spectrum for $KPdPS_4$.

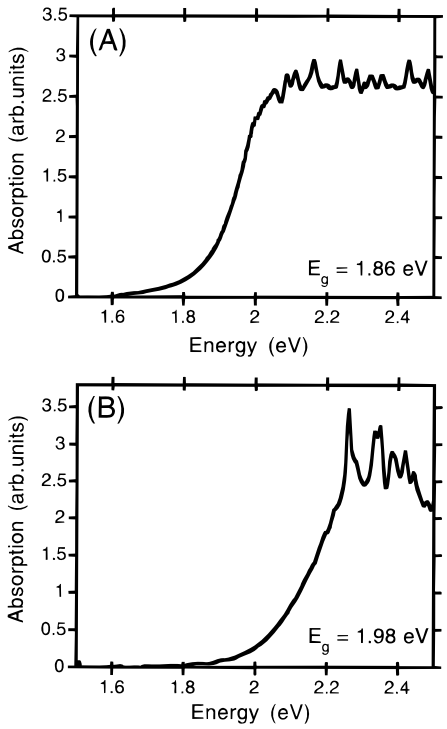

Figure 8. (A) Single-crystal optical transmission data converted to absorption data for $Cs_4Pd(PSe_4)_2$ and plotted as absorption vs energy. (B) Single-crystal optical transmission data converted to absorption data for $Cs_{10}Pd(PSe_4)_4$ and plotted as absorption vs energy.

compound $Pb_3(PQ_4)_2$ is three-dimensional, $APbPSe_4$ is 2-D, and $A_4Pb(PSe_4)_2$ is 1-D.

We have learned from our investigations in chalcophosphate fluxes that the P/S chemistry varies significantly from the corresponding P/Se chemistry even under the same experimental conditions. Thus isostructural S and Se compounds are not often obtained. Strangely, the isotypic nature of $[Pd(PS_4)_2]^{4-}$ and $[Pd(PSe_4)_2]^{4-}$ is somewhat of an exception. A significant reason for the difference is the distinct chemical redox behavior of P in thio and seleno enviroments. In A/P/S fluxes, the tendency of P to adopt mostly a P^{5+} state is greater than it is in A/P/Se fluxes, where P^{4+} centers are more frequently encountered. So anions such as $[PS_4]^{3-}$ and $[P_2S_7]^{4-}$ are common, while the $[P_2Se_6]^{4-}$, with a P^{4+} species, has been found in many A/M/P/Se phases. This behavior is consistent with the greater reducing power of Se^{2-} than of S^{2-}. Perhaps this could explain why $Pd_3(PS_4)_2$ exists but $Pd_3(PSe_4)_2$ has not been reported. $[PSe_4]^{3-}$ is the next more frequent anion, but in many systems one has to employ much more basic flux conditions (i.e., high A_2Se content) to form phases which incorporate it. On the other hand, we have yet to observe a flux-prepared compound with the $[P_2S_6]^{4-}$ anion. The only compounds containing the latter have been prepared with direct combination reactions. When compounds between S and Se contain the same $[P_xQ_y]^{n-}$ anions, they tend to be isostructural, as for example in the case of $KTiPSe_5$[7a] and $KTiPS_5$.[28]

(b) Spectroscopy. The solid-state UV/vis diffuse reflectance spectra of the sulfur compounds reveal sharp optical absorptions consistent with semiconductors. The compounds exhibit absorption edges associated with band gaps of 2.00 eV for **I** and 1.88 eV for **IV**; see Figure 7. The transparent, well-formed crystals of **II** and **III** were suitable for single-crystal optical transmission measurements, Figure 8. Both compounds exhibit absorption edges from which the band gaps can be estimated at 1.86 eV for **II** and 1.98 eV for **III**. The energy gap of **II** is smaller than that of the sulfur analog **I**, as one would expect for the larger selenium atom. In addition, going from the molecular compound **I** to the chainlike compound **II**, the "localized" energy levels give rise to more dispersed bands and lower energy gaps. Some higher energy absorptions are resolved at 4.26, 3.21, 2.51 eV (for **I**) and at 2.43, 4.36 eV (for **IV**) that can be assigned as S → M charge transfer transitions. Table 14 summarizes the band gaps and melting points of **I**−**VI**.

Table 14. Optical Band Gaps and Melting Point Data

formula	E_g, eV	mp, °C	formula	E_g, eV	mp, °C
$K_4Pd(PS_4)_2$	2.00	530[a]	$KPdPS_4$	1.88	750[a]
$Cs_4Pd(PSe_4)_2$	1.86	602	$Cs_2PdP_2Se_6$	1.60	615[a]
$Cs_{10}Pd(PSe_4)_4$	1.98	644			

[a] Incongruent melting.

Compounds **I**−**III** dissolve in a crown ether 18C6 solution in DMF, as described before.[11] The solution of **I** is blue whereas the solutions of **II** and **III** are light green. The DMF/complexant solution of **I** gave an absorption at ∼617 nm (2.01 eV), suggesting the presence of polysulfide ions. Compounds **II** and **III** gave similar solution UV/vis spectra. For **II**, three absorptions appear at ∼595 nm (2.08 eV), ∼487 nm (2.55 eV), and ∼353 nm (3.52 eV), and for **III**, two absorptions appear at ∼442 nm (2.81 eV) and ∼348 nm (3.57 eV). Because the solution spectra are dramatically different from those in the solid state, it is evident that the complexes decompose in solution to give Se_x^{2-} anions. Compound **I** is also soluble in water, resulting in an orange solution with a strong absorption at ∼498 nm (2.49 eV). To test whether the complex is stable in water, we compared the Raman spectra in solution with that in the solid state, Figure 9. The two spectra display absorptions at ∼155 and ∼184 cm^{-1} (Pd−S vibrations) and at ∼218, 236, 249, 298, 338, 417, 471, 576, and 598 cm^{-1} (P−S vibrations of the $[PS_4]^{3-}$ group).[8b] Apart from differences in the relative intensity of the absorptions, the two spectra appear identical, suggesting that complex **I** remains intact in water.

(28) Do, J.; Lee, K.; Yun, H. *J. Solid State Chem.* **1996**, *125*, 30.

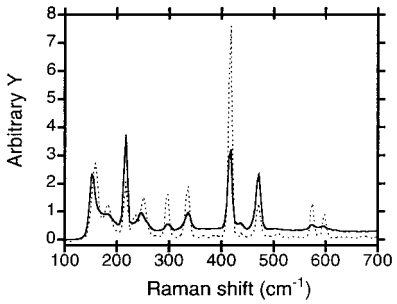

Figure 9. Water solution (solid line) and solid-state (dashed line) Raman spectra of $K_4Pd(PS_4)_2$.

The far-IR spectra of **I** and **IV** display absorptions in the 552−400 cm^{-1} range which are tentatively assigned to the P−S vibrational stretching modes by analogy with the spectra of $AuPS_4$,[29] MPS_4 (M = In, Ga, Ba),[30] and $KNiPS_4$.[25] Absorptions below 400 cm^{-1} are assigned to S−P−S bending modes and Pd−S vibrations.[29] The far-IR spectra of **II** and **III** display the characteristic absorptions of the $[PSe_4]^{3-}$ unit,[1,6] but they also contain an absorption at 387 cm^{-1} which can be tentatively assigned to Se−P−Se bending modes or Pd−Se vibrations; see Table 15. The far-IR spectrum of **VI** displays the characteristic absorptions of the $[P_2Se_6]^{4-}$ unit.[1]

(c) Thermal Analysis. Differential thermal analysis (DTA) data followed by XRD analysis of the residues, show that **II** and **III** melt congruently at 602 and 644 °C, respectively. On the other hand, **I**, **IV**, and **VI** decompose upon heating. **I** yields a mixture of **I** and an unidentified phase. **IV** yields a mixture of **IV** and amorphous $K_xP_yS_z$. **VI** yields a mixture of **VI** and amorphous $Cs_xP_ySe_z$.

Concluding Remarks

The following are the principal findings and conclusions of this study. The synthesis of the first members of the A/Pd/P/Q family from the polychalcophosphate $A_x[P_yQ_z]$ fluxes was achieved. Because it has yielded new compounds in literally every area of the periodic table, from main group metals[2−6,11] and early[7a] and late[1,7b,8] transition metals to lanthanides[6,10] and actinides,[9] undoubtedly the polychalcophosphate flux provides the best synthetic route to P−Q compounds. By variation of the basicity conditions in the flux, access to both molecular and solid-state compounds is possible. The Pd chalcophosphate chemistries appear to be similar in both the cases of sulfur and selenium, unlike the situation with other metals. For the case of $[PQ_4]^{3-}$ group, we observe a new family of compounds with the general formula $(A_3PQ_4)_n[Pd_3(PQ_4)_2]_m$. The success in transforming molecular chalcophosphates to solid-state compounds opens new horizons in this chemistry, and mixed-metal quinternary $A_xM_aM'_bP_yQ_z$ compounds might be feasible.[31]

Table 15. Infrared Data (cm^{-1}) for **I**−**IV**

$K_4Pd(PS_4)_2$	$Cs_4Pd(PSe_4)_2$	$Cs_{10}Pd(PSe_4)_4$	$KPdPS_4$	$Cs_2PdP_2Se_6$
516	469	467	552	490
416	448	451	325	442
329	436	436	309	306
312	405	387	265	
274	387		239	
255				
201				
185				

Acknowledgment. Financial support from National Science Foundation Grant DMR-9527347 is gratefully acknowledged. M.G.K. is an A. P. Sloan Foundation, and a Camille and Henry Dreyfus Teacher-Scholar, 1993−1998. This work used the SEM facilities of the Center for Electron Optics at Michigan State University.

Supporting Information Available: Tables of experimental crystallographic details for **I**−**VI**, anisotropic and isotropic thermal parameters of all atoms for **I**−**VI**, and calculated and observed X-ray powder patterns for **I**, **II**, and **IV** (18 pages). Ordering information is given on any current masthead page.

IC970593N

(29) Pätzmann, U.; Bröckner, W..; Cyvin, B. N.; Cyvin, S. J. *J. Raman Spectrosc.* **1986**, *17*, 257.
(30) D'ordyai, V. S.; Galagovets, I. V.; Peresh, E. Yu.; Voroshilov, Yu. V.; Gerasimenko, V. S.; Slivka, V. Yu. *Russ. J. Inorg. Chem. (Engl. Transl.)* **1979**, *24*, 1603.
(31) Chondroudis, K.; Kanatzidis, M. G. Submitted for publication.